Journal of Turbomachinery. Received July 17, 2022;
Accepted manuscript posted August 25, 2022. doi:10.1115/1.4055449

PLUME MODEL FOR BUOYANCY-INDUCED FLOW AND HEAT TRANSFER IN CLOSED ROTATING CAVITIES

Hui Tang* J. Michael Owen

Department of Mechanical Engineering
University of Bath
Bath, BA2 7AY
United Kingdom
*E-mail: h.tang2@bath.ac.uk

ABSTRACT

The radial clearance between the rotating blades and stationary casing of a gas turbine compressor depends on the radial growth of the rotating discs to which the blades are attached, and this growth depends on the buoyancy-induced flow and heat transfer in the air-filled cavities between adjacent discs. In some engines, the cavities are sealed, which creates a closed rotating cavity. A theoretical model has been developed to calculate the radial distribution of the temperature of the disc in a closed rotating cavity. The principal assumptions are that the convective heat transfer from the hot shroud to the cold hub of the cavity is via plumes of fluid in which the cold fluid moves radially outward, and the hot fluid inward, inside an inviscid quasi-axisymmetric core of rotating fluid. The fluid core is surrounded by boundary layers on all rotating surfaces, with free-convection layers on the surfaces of the shroud and hub and laminar Ekman layers on the surface of the discs. In addition to the convection, heat is transferred by one-dimensional radial conduction in the rotating discs. Using the model, equations have been derived to calculate the radial distribution of temperature in the discs and fluid core. These equations reveal that the non-dimensional temperatures for the disc and core, θ_d and θ_c, are controlled by three independent non-dimensional parameters: Re_ϕ, $\beta\Delta T$ and χ, the rotational Reynolds number, the buoyancy parameter, and the compressibility parameter, respectively. The compressibility parameter is defined as $\chi \overset{\text{def}}{\equiv} \mathrm{Ma}^2/\beta\Delta T$ where Ma is a Mach number, and χ is shown to strongly affect the radial distribution of the core temperatures. There will be a critical value of χ at which the core temperature equals that of the heated shroud. For a closed cavity with adiabatic discs and $x_a = 0.5$, the critical value is 6.7. Above this critical value, stratification is expected to occur and heat transfer from the shroud to the core will be by conduction rather than by convection. The theoretical model predicts radial distributions of temperatures in the discs and fluid core that are in good agreement with the experimentally derived values in a companion paper.

1 INTRODUCTION

One of the major problems facing gas-turbine designers is the control of the clearance between the blades and casing of the high-pressure compressor. This clearance depends strongly on the radial growth of the compressor discs to which the blades are attached, and this in turn depends not only on the level but also on the radial distribution of the temperature of the discs. Calculation of the disc temperature is a conjugate problem: the temperature depends on the flow structure inside the air-filled cavity between adjacent discs and the flow depends on the disc temperature. Although in principle the flow, which is three-dimensional unsteady and unstable, can be calculated using computational fluid dynamics (CFD), this is very expensive and time consuming. In practice, designers tend to rely on empirical correlations and on simple models to calculate the disc temperatures.

In aero-engines, the cavities between the discs are open at the bore, which means that there is interaction between the axial throughflow at the bore of the discs and the flow inside the cavity. In some gas turbines, see Figure 1, some cavities are closed, and these are the subject of this paper.

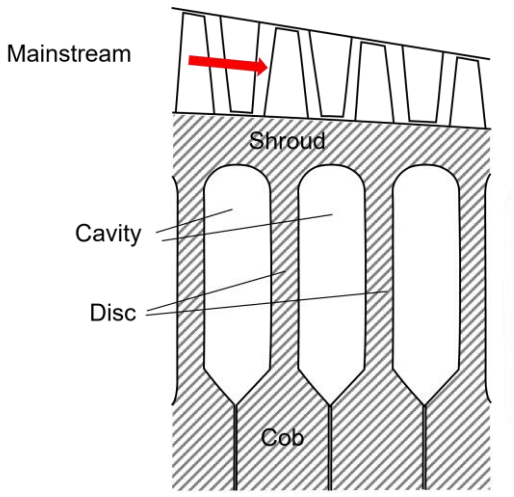

Figure 1: Cutaway of a typical industrial gas turbine compressor.

Journal of Turbomachinery. Received July 17, 2022;
Accepted manuscript posted August 25, 2022. doi:10.1115/1.4055449

The review of buoyancy-induced flow by Owen and Long [1] includes details of both open and closed rotating cavities, and some of the relevant details for closed cavities is included here. The closest stationary analogue for a closed rotating cavity is free convection between horizontal plates in a gravitational field, as shown in Figure 2 [2]. For this stationary case, the Rayleigh number, Ra', is defined as

$$\mathrm{Ra}' \stackrel{\text{def}}{=} \mathrm{Pr}\beta\Delta T\frac{gd^3}{\nu^2} \tag{1}$$

where d is the vertical distance between the plates and $\Delta T = T_H - T_C$. When the lower surface is hotter than the upper one, the fluid becomes unstable and at a critical Rayleigh number the flow develops into a series of counter-rotating vortices, as illustrated in Figure 2. This buoyancy-induced flow is referred to as Rayleigh-Bénard convection, and the value of the critical Rayleigh number at which convection starts is Ra'_{crit} = 1708. For these stationary systems, the Nusselt number can be correlated in terms of a *single parameter*, usually the Rayleigh number or the Grashof number, in which the buoyancy parameter $\beta\Delta T$ is the only independent variable.

There are several important differences for buoyancy-induced flow in a rotating fluid. In particular, in a closed rotating cavity, convection can only occur when the outer cylindrical surface (referred to as the shroud) is hotter than the inner surface (the hub). At large rotational speeds in a rotating cavity, where

$$\Omega^2 a \gg g \tag{2}$$

and a is the inner radius of the cavity; the gravitational acceleration is negligible compared with the centripetal acceleration. Unlike gravity, the centripetal acceleration is an independent variable which, together with the buoyancy parameter, $\beta\Delta T$, makes this a *two-parameter* problem. (It is shown below that, owing to compressibility effects, this is actually a *three-parameter* problem.) It is also a *conjugate problem*: the heat transfer from the discs depends upon the flow structure in the core, and vice versa.

The Grashof number, Gr, for rotating fluids is often defined by

$$\mathrm{Gr} \stackrel{\text{def}}{=} \mathrm{Re}_\phi{}^2\beta\Delta T \tag{3a}$$

and the Rayleigh number is given by

$$\mathrm{Ra} = \mathrm{GrPr} \tag{3b}$$

where Pr is the Prandtl number. The Reynold number Re_ϕ is defined as

$$\mathrm{Re}_\phi \stackrel{\text{def}}{=} \frac{\Omega b^2}{\nu} \tag{4}$$

As far as the authors are aware, the critical value, Ra_{crit}, for buoyancy-induced flow to occur in a rotating fluid has not been determined.

Under steady-state conditions, the shroud of the compressor is hotter than the hub, and buoyancy-induced flow occurs inside the cavity between adjacent compressor discs. However, under engine decelerations, the shroud can become colder than the hub, and this suppresses buoyancy effects. Under these conditions, stratified flow occurs in which convection is replaced by conduction inside the fluid core. This can make a significant difference to the temperature distribution and stresses inside the compressor discs.

Outside the boundary layers that exist on the rotating surfaces of the closed cavity, there is a rotating core of inviscid fluid in which Coriolis forces are necessary for radial flow to occur. These forces are created by cyclonic and anticyclonic vortices within the cavity, as illustrated in Figure 3. The anti-cyclonic vortex generates a positive pressure and the cyclonic vortex generates a negative pressure; the circumferential pressure differences between these vortices provides the necessary Coriolis forces for radial outflow (of the cold fluid) and inflow (of the hot fluid) to occur inside the core. It was shown by Owen [3] that the number of vortex pairs inside the core can be explained by the maximum entropy production theorem, in which self-organising systems that are far from equilibrium seek to maximise the rate of entropy production; for a closed rotating cavity, this corresponds to maximising the heat transfer. Evidence for these flow structures is given in many experimental [[4]-9] and computational [10-13] studies.

This paper details the derivation of a physically-based mathematical model, referred to as the *plume model*, which can be used to calculate the disc temperature and heat flux in a closed rotating cavity. Section 2 explains the principal assumptions for the model and presents the so-called linear equations for rotating fluids. Section 3 shows the derivation of the equations for the temperatures in the plumes, core and discs. Section 4 shows the derivations of the radial and circumferential pressures in the core and relates these to the mass flow rate in the plumes. A parametric study showing the effect of the compressibility parameter, Reynolds number and buoyancy parameter on the temperatures and heat fluxes in the cavity is presented in Section5, and the main conclusions are given in Section 6.

A companion paper [14] includes experimental measurements in a closed-cavity rig and compares these with predictions from the plume model.

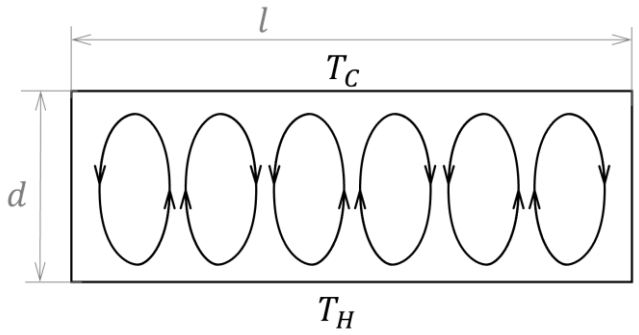

Figure 2: Free convection between horizontal plates.

Journal of Turbomachinery. Received July 17, 2022;
Accepted manuscript posted August 25, 2022. doi:10.1115/1.4055449

2 PRINCIPAL ASSUMPTIONS AND LINEAR EQUATIONS

2.1 Assumptions

Figure 3 shows the simplified flow structure assumed for the model in which the temperature of the shroud (the outer cylindrical surface of the cavity) is higher than that of the hub (the inner cylindrical surface). Figure 3a shows the flow structure in the r-ϕ plane of the inviscid fluid core between the discs where a plume of cold fluid flows radially outward and one of hot fluid flows inward. The plumes, which are separated by contra-rotating cyclonic and anticyclonic vortices, rotate at virtually the same speed as the fluid core. It is also assumed that the mass flow in the cold plume equals that in the hot one and that the mass flow rate is invariant with radius. The fluid core is assumed to be quasi-axisymmetric, with a large radial pressure gradient to create the centripetal acceleration of the rotating fluid; in addition, a small circumferential pressure gradient is required to create the Coriolis force for the plume flow.

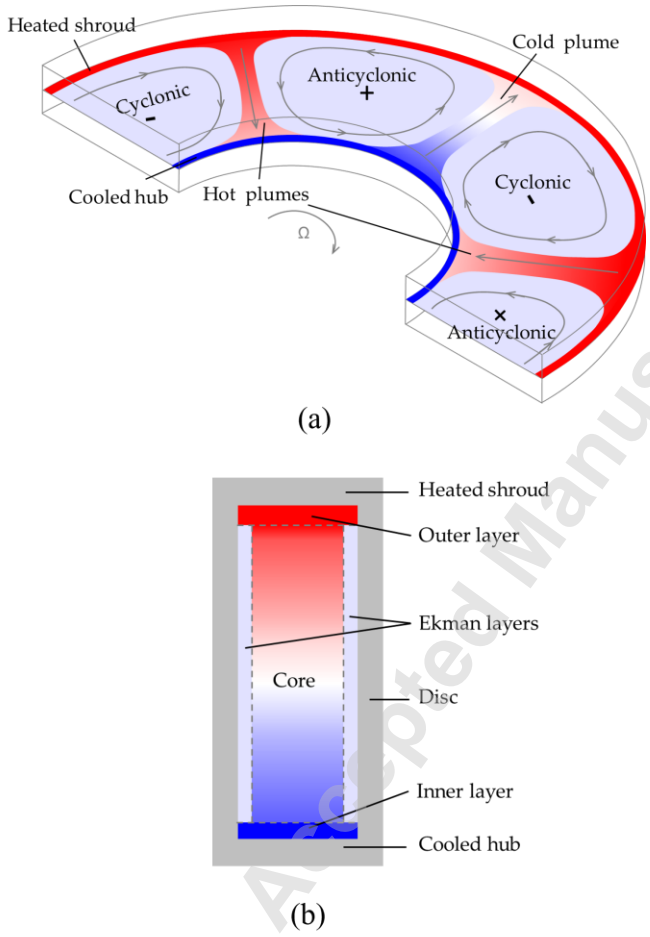

Figure 3: Simplified representation of buoyancy-induced flow inside a closed rotating cavity, showing the *r*-ϕ plane (a) and the *r*-*z* plane (b).

As shown in Figure 3b, the core is surrounded by boundary layers on all rotating surfaces, and laminar Ekman-layer flow is assumed to occur in the boundary layers on the discs. Ekman-layer flow depends on differential rotation between the discs and the core, although in closed cavities the speed difference is very small. (Even at the high rotational speeds found in engines, the Coriolis forces can be large enough to suppress turbulence, and there is considerable evidence in the papers to support the assumption of laminar Ekman layer flow [15-21].)

Heat transfer at the outer radius, $r = b$, is assumed to occur in a thin layer by free convection to the fluid and by one-dimensional conduction to the discs. Heat transfer at the inner radius, $r = a$, occurs in a thin layer by free convection from the fluid (including the heat transferred from the discs to the core) and by conduction from the discs. At the outer radius, the convective heat transfer is assumed to create the temperature difference between the hot and cold plumes; the converse is assumed for the inner radius. An overall heat balance is used to close the derived system of equations.

Some other simplifying assumptions are introduced in the relevant places below. Subscripts *c*, *d*, *h*, and *s* are used respectively below to denote the circumferentially-averaged fluid core, discs, hub, and shroud; subscripts $\hat{p}$ and $\check{p}$ refer respectively to the outflowing (cold) and inflowing (hot) plumes.

2.2 Linear equations for rotating fluids

When the Coriolis terms in the boundary layer equations of a rotating fluid are much greater than the inertial terms, the so-called *linear equations* can be used to simplify the analysis (see, for example, [22] or [23]). For incompressible laminar flow in the Ekman layers, and in a rotating frame of reference, these equations reduce to

$$2\rho\Omega(v - v_\infty) = -\mu\frac{\partial^2 u}{\partial z^2} \tag{5a}$$

$$2\rho\Omega(u - u_\infty) = \mu\frac{\partial^2 v}{\partial z^2} \tag{5b}$$

where u_∞ and v_∞ are the local radial and tangential component of the relative velocity in the core. The solution to these equations is

$$u - u_\infty = -u_\infty e^{-\varphi}\cos\varphi - v_\infty e^{-\varphi}\sin\varphi \tag{6a}$$

$$v - v_\infty = -v_\infty e^{-\varphi}\cos\varphi + u_\infty e^{-\varphi}\sin\varphi \tag{6b}$$

where φ, the angle in the axial direction, is given by

$$\varphi = \frac{z}{\delta} \tag{7a}$$

and

$$\delta = \sqrt{\frac{\mu}{\rho\Omega}} \tag{7b}$$

The effective thickness of the Ekman layer, δ^*, is based on the value of z where $\varphi = \pi$, so that

Journal of Turbomachinery. Received July 17, 2022;
Accepted manuscript posted August 25, 2022. doi:10.1115/1.4055449

$$\delta^* = \pi\delta = \pi\sqrt{\frac{\mu}{\rho\Omega}} \tag{8}$$

For the circumferentially-averaged core, $u_c \approx 0$, and a quasi-axisymmetric form of eqs. (6a & 6b) can be written as

$$u = -v_c e^{-\varphi}\sin\varphi \tag{9a}$$

$$v - v_c = -v_c e^{-\varphi}\cos\varphi \tag{9b}$$

If the inertial and dissipation terms are also neglected in the laminar energy equation, the temperature inside the Ekman layer reduces to

$$\frac{\partial^2 T}{\partial z^2} = 0 \tag{10}$$

The linear temperature distribution inside the Ekman layer can therefore be approximated by

$$T - T_\infty = (T_d - T_\infty)\left(1 - \frac{z}{\delta^*}\right) \tag{11}$$

and the heat flux from the disc to the core, q_d, can be calculated by

$$q_d = -k\frac{\partial T}{\partial z} = \frac{k}{\delta^*}(T_d - T_c) \tag{12}$$

Note that the disc temperature is considered to be axisymmetric, and T_c is the circumferentially-averaged temperature in the fluid core, hence

$$T_c = \frac{1}{2\pi}\int_0^{2\pi} T_\infty d\phi \tag{13}$$

where ϕ is the angle in the circumferential direction.

The heat transfer coefficient for the disc, h_d, is therefore given by

$$h_d = \frac{q_d}{T_d - T_c} = \frac{k}{\delta^*} \tag{14}$$

where k is the thermal conductivity of the air.

The linear equation for the angular momentum in a rotating inviscid fluid is given by

$$2\rho\Omega u_\infty = \frac{1}{r}\frac{\partial p}{\partial \phi} \tag{15}$$

This equation is used below for flow in the plumes, where the radial component of velocity is proportional to the mass flow rate.

3 CALCULATION OF TEMPERATURES IN PLUMES, CORE AND DISCS

3.1 Plume temperatures

The differential steady-flow energy equation, derived from the first law of thermodynamics, can be applied to the plumes illustrated in Figure 3. The sum of the mass flow rates in all the hot plumes, $\dot{m}$, is assumed to be equal to the sum of mass flow rates in all the cold plumes.

In the closed-cavity experiments of Jackson et al. [4], the relative difference between the speed of the core and that of the discs was less than 1%. For simplicity, in all the equations derived below it is assumed that the difference between the angular speeds of the core and discs is negligible and consequently $U_\phi = \Omega$r.

For the outward flowing cold plumes

$$d\dot{Q}_{\hat{p}} + d\dot{W}_{\hat{p}} = \dot{m}dH \tag{16}$$

where $\dot{Q}_{\hat{p}}$ and $\dot{W}_{\hat{p}}$ are the heat and work terms and H is the total enthalpy. As it is assumed that $U_\phi^2 \gg U_r^2$ and U_z^2, H is given by

$$H = C_p T_{\hat{p}} + \frac{1}{2}U_\phi^2 \tag{17}$$

where H is the total enthalpy.

It is assumed that the circumferential variation of the disc temperature is negligible and that heat is transferred to either of the hot and cold plumes through half the disc surface area. The elemental heat transfer from the axisymmetric upstream and downstream discs to the cold plumes, $d\dot{Q}_{\hat{p}}$, is therefore given by

$$d\dot{Q}_{\hat{p}} = 2\pi h_d(T_d - T_{\hat{p}})\,rdr \tag{18}$$

The elemental rate of work done by the circumferential pressure gradient on the plume, $d\dot{W}_{\hat{p}}$, is given by

$$d\dot{W}_{\hat{p}} = \dot{m}\Omega\frac{d(rU_\phi)}{dr}dr = 2\dot{m}\Omega^2 rdr \tag{19}$$

The elemental total enthalpy, dH, is given by

$$dH = d\left(c_p T_{\hat{p}} + \frac{1}{2}U_\phi^2\right) = c_p\left(\frac{dT_{\hat{p}}}{dr}\right)dr + \Omega^2 rdr \tag{20}$$

Eq. (16) then becomes

$$\frac{dT_{\hat{p}}}{dr} = \frac{2\pi h_d(T_d - T_{\hat{p}})r}{c_p\dot{m}} + \frac{\Omega^2 \mathrm{r}}{c_p} \tag{21}$$

For the *hot plume*, it is appropriate to use the inflow direction, where

$$\eta = \mathrm{b} - \mathrm{r} \tag{22}$$

It follows that

$$d\dot{Q}_{\check{p}} = 2\pi h_d(T_d - T_{\check{p}})rd\eta \tag{23a}$$

$$d\dot{W}_{\check{p}} = -2\dot{m}\Omega^2 rd\eta \tag{23b}$$

$$dH = c_p\left(\frac{dT_{\check{p}}}{d\eta}\right)d\eta - \Omega^2 rd\eta \tag{23c}$$

Hence

$$\frac{dT_{\check{p}}}{d\eta} = \frac{2\pi h_d(T_d - T_{\check{p}})r}{c_p\dot{m}} - \frac{\Omega^2 r}{c_p} \tag{24a}$$

or

Journal of Turbomachinery. Received July 17, 2022;
Accepted manuscript posted August 25, 2022. doi:10.1115/1.4055449

$$\frac{dT_{\check{p}}}{dr} = -\frac{2\pi h_d(T_d - T_{\check{p}})r}{c_p\dot{m}} + \frac{\Omega^2 r}{c_p} \quad (24b)$$

3.2 Core temperature

It is assumed that

$$T_c = \frac{1}{2}(T_{\hat{p}} + T_{\check{p}}) \quad (25)$$

The elemental heat transfer from both discs to the fluid core, $d\dot{Q}_d$, can be given by

$$d\dot{Q}_d = d\dot{Q}_{\check{p}} + d\dot{Q}_{\hat{p}} = 4\pi r h_d(T_d - T_c)dr \quad (26)$$

Using eqs. (21), (24) and (25) it follows that

$$\frac{dT_c}{dr} = \frac{\pi h_d(T_{\check{p}} - T_{\hat{p}})r}{c_p\dot{m}} + \frac{\Omega^2 r}{c_p} \quad (27)$$

In the outer layer, at r = b, the heat flow from the shroud, $\dot{Q}_s$, equals the enthalpy difference between the hot and cold plumes at r = b, so that

$$\dot{Q}_s = \dot{m}c_p(T_{\check{p}} - T_{\hat{p}})_b \quad (28)$$

also

$$\dot{Q}_s = 2\pi s b h_s(T_s - T_{c,b}) \quad (29)$$

where s is the axial width of the shroud, and h_s , the heat transfer coefficient for the shroud, can be found from an appropriate free-convection correlation.

The combined heat flow rate, $\dot{Q}$, from the shroud and discs to the core between the radii r and b is given by

$$\dot{Q} = 2\pi s b h_s(T_s - T_{c,b}) + 4\pi\int_r^b h_d(T_d - T_c)r dr \quad (30)$$

This equals the enthalpy difference between the plumes, so that

$$\dot{Q} = \dot{m}c_p(T_{\check{p}} - T_{\hat{p}}) \quad (31)$$

It follows that

$$T_{\check{p}} - T_{\hat{p}} = \frac{2\pi}{c_p\dot{m}}\left(s b h_s(T_s - T_{c,b}) + 2\int_r^b h_d(T_d - T_c)r dr\right) \quad (32)$$

Eq. (27) then becomes

$$\frac{dT_c}{dr} = \frac{2\pi^2 h_d r}{(c_p\dot{m})^2}\left(s b h_s(T_s - T_{c,b}) + 2\int_r^b h_d(T_d - T_c)r dr\right) + \frac{\Omega^2 r}{c_p} \quad (33)$$

The first term on the right-hand side of eq. (33) is proportional to the combined heat flow rate from the discs and shroud to the core. The second term is proportional to the adiabatic core temperature given by Owen and Tang [15].

Similar to that from the shroud, the heat flow rate leaving the hub, $\dot{Q}_h$, equals the enthalpy difference between the hot and cold plumes at r = a, so that

$$\dot{Q}_h = \dot{m}c_p(T_{\check{p}} - T_{\hat{p}})_a \quad (34)$$

Also

$$\dot{Q}_h = 2\pi s a h_h(T_{c,a} - T_h) \quad (35)$$

where h_h is the heat transfer coefficient for the hub, which can be determined using an appropriate free-convection correlation. Therefore, at r = a, the combined heat flow rate from the shroud and discs should be equal to that to the hub. As discussed in Section 5, this heat balance can be used to determine the core temperature at r = a, $T_{c,a}$.

3.3 Disc temperature

It was shown by Tang et al. [24] that the disc temperature could be calculated using the circular-fin equation, which can be written as

$$\frac{d^2T_d}{dr^2} + \frac{1}{r}\frac{dT_d}{dr} - \frac{2h_d}{t_d k_d}(T_d - T_c) = 0 \quad (36)$$

where t_d and k_d are the thickness and the thermal conductivity of the discs. Equations (33) and (36) express the relationship between the coupled temperatures of the core and disc, and details about how their solution are given in Section 5.

4 PRESSURE DISTRIBUTION IN CORE

4.1 Radial pressure distribution

For radial equilibrium in the inviscid core, the average pressure and density are related by

$$\frac{\partial p_c}{dr} = \rho_c\Omega^2 r \quad (37)$$

In addition, the pressure and density are related to the temperature in the core by the perfect gas law where

$$\frac{p_c}{\rho_c} = RT_c \quad (38)$$

It follows that

$$\frac{\partial p_c}{p_c} = \frac{\Omega^2}{R}\frac{r}{T_c}dr \quad (39)$$

Hence

$$\frac{p_c}{p_{c,a}} = exp\left(\frac{\Omega^2}{R}\int_a^r \frac{\mathrm{r}}{T_c}dr\right) \quad (40)$$

In a closed cavity, the mass of air, m, is related to the volume, V, by

$$m = \rho_o V \quad (41)$$

where

$$\rho_o = \frac{p_o}{RT_o} \quad (42)$$

the subscript o denoting the initial conditions for an isothermal stationary cavity. For the rotating cavity, neglecting the thin boundary layers on the surfaces, the elemental mass is given by

$$dm = 2\pi r s\rho_c dr \quad (43)$$

Hence

$$m = \bar{\rho_c}V \quad (44)$$

Journal of Turbomachinery. Received July 17, 2022;
Accepted manuscript posted August 25, 2022. doi:10.1115/1.4055449

where the circumferentially-averaged density in the closed cavity can be calculated using

$$\overline{\rho_c} = \frac{2}{b^2 - a^2}\int_a^b \rho_c r dr = \rho_o \tag{45}$$

It follows using eq. (37) that

$$p_{c,b} - p_{c,a} = \frac{\Omega^2(b^2 - a^2)}{2}\rho_o \tag{46}$$

Also, it follows from eq. (40) that

$$p_{c,b} = exp\left(\frac{\Omega^2}{R}\int_a^b \frac{r}{T_c}dr\right)p_{c,a} \tag{47}$$

Hence

$$p_{c,a} = \frac{\Omega^2(b^2 - a^2)}{2\left(\exp\left(\frac{\Omega^2}{R}\int_a^b \frac{r}{T_c}dr\right) - 1\right)}\rho_o \tag{48}$$

That is, for any rotational speed, the pressure and density in the heated cavity depends on the initial conditions of these parameters in the stationary isothermal cavity and on the radial temperature distribution of the core. It should also be noted that it is possible that $p_{c,a} < p_o$.

4.2 Circumferential pressure distribution

The cyclonic and anticyclonic vortices in the core create the circumferential pressure distribution that provides the Coriolis forces for the radial flow in the plumes. The linear angular momentum equation for the inviscid flow in the cold plume can be written as

$$2\rho_{\hat{p}}\Omega u_{\hat{p}} = -\frac{1}{r}\frac{\partial p}{\partial \phi} \tag{49}$$

For a single plume, denoted by the subscript i, eq. (49) can be integrated to give

$$\Delta p_i = 2\Omega \mathrm{r}\int_0^{\Delta\phi_i} \rho_{\hat{p}} u_{\hat{p}} \mathrm{d}\phi = 2\Omega\overline{\rho_{\hat{p}} u_{\hat{p}}}\ \mathrm{r}\Delta\phi_i \tag{50}$$

where $\overline{\rho_{\hat{p}} u_{\hat{p}}}$ is an average value of the mass flux in the plume, $\Delta\phi_i$ is the effective angular difference and Δp_i is the effective pressure difference between the centre of the cyclonic and anticyclonic vortices.

The mass flow rate in a single plume can be calculated by

$$\dot{m}_{\hat{p},i} = \overline{\rho_{\hat{p}} u_{\hat{p}}} A_i = \frac{s}{2\Omega}\Delta p_i \tag{51}$$

Ignoring the thickness of the Ekman layers, the area $A_i = sr\Delta\phi_i$, s being the axial width of the cavity. The total mass flow rate of n pairs of plumes can be calculated by

$$\dot{m} = \sum_{i=1}^{n} \dot{m}_{\hat{p},i} = n\frac{s}{2\Omega}\Delta p \tag{52}$$

Note that the strengths of different vortex pairs are assumed to be the same, hence $\Delta p = \Delta p_i$. As $\dot{m}_{\hat{p}}$ is invariant with r, eq. (52) implies that Δp must also be invariant with r. This equation is used for the correlation for $\dot{m}_{\hat{p}}$ obtained in the companion paper [14].

5 CALCULATION OF CORE AND DISC TEMPERATURES

5.1 Non-dimensionalisation

The parametric study is used to show the theoretical effect of the compressibility parameter χ, the rotational Reynolds number Re_ϕ and the thermal conductivity ratio of the air k to the discs k_d on the nondimensional core and disc temperatures, θ_c and θ_d.

The rotational Reynolds number is defined in eq. (4). The buoyancy parameter $\beta\Delta T$ and the Mach number Ma are defined as

$$\beta\Delta T \stackrel{\text{def}}{=} \frac{\Delta T}{(T_b + T_a)/2} \tag{53}$$

$$\mathrm{Ma} \stackrel{\text{def}}{=} \frac{\Omega b}{c} \tag{54}$$

where c is the speed of sound and can be calculated from

$$c = \sqrt{\gamma R(T_b + T_a)/2} \tag{55}$$

The relationship between Ma and Re_ϕ is given by

$$\mathrm{Ma} = \frac{\mu}{\rho_o c b}\mathrm{Re}_\phi \tag{56}$$

The disc, shroud and hub Nusselt number can be defined as

$$\mathrm{Nu}_d \stackrel{\text{def}}{=} \frac{h_d b}{k} \tag{57a}$$

$$\mathrm{Nu}_s \stackrel{\text{def}}{=} \frac{h_s(s/2)}{k} \tag{57b}$$

$$\mathrm{Nu}_h \stackrel{\text{def}}{=} \frac{h_h(s/2)}{k} \tag{57c}$$

Using eqs. (4), (8) and (14), the disc Nusselt number can be calculated using

$$\mathrm{Nu}_d = \frac{1}{\pi}\mathrm{Re}_\phi^{1/2} \tag{58}$$

The plume mass flow parameter and the pressure parameter are

$$C_w \stackrel{\text{def}}{=} \frac{\dot{m}}{\mu s} \tag{59}$$

$$C_p \stackrel{\text{def}}{=} \frac{\Delta p}{\rho_o \Omega^2 b^2} \tag{60}$$

The non-dimensional core and disc temperatures are defined as

$$\theta_c \stackrel{\text{def}}{=} \frac{T_c - T_a}{\Delta T} \tag{61}$$

and

Journal of Turbomachinery. Received July 17, 2022;
Accepted manuscript posted August 25, 2022. doi:10.1115/1.4055449

$$\theta_d \stackrel{\text{def}}{\equiv} \frac{T_d - T_a}{\Delta T} \tag{62}$$

where $\Delta T = T_b - T_a$, and T_a and T_b are the disc temperature at $r = a$ and $r = b$. Therefore, $\theta_{d,a} = 0$ and $\theta_{d,b} = 1$.

Eqs. (33) and (36) can then be presented in non-dimensional form by

$$\frac{d\theta_c}{dx} = 4\pi^2 x\lambda\left[1 - \theta_{c,b} + \int_x^1 x\frac{\mathrm{Nu}_d}{\mathrm{Nu}_s}(\theta_d - \theta_c)dx\right] + (\gamma - 1)x\chi \tag{63}$$

and

$$\frac{d^2\theta_d}{dx^2} + \frac{1}{x}\frac{d\theta_d}{dx} - \mathrm{Bi}(\theta_d - \theta_c) = 0 \tag{64}$$

where

$$x \stackrel{\text{def}}{\equiv} r/b \tag{65}$$

$$\lambda \stackrel{\text{def}}{\equiv} \left(\frac{b}{s}\right)^2 \frac{\mathrm{Nu}_d \mathrm{Nu}_s}{C_w^2 \mathrm{Pr}^2} \tag{66}$$

$$\chi \stackrel{\text{def}}{\equiv} \frac{\mathrm{Ma}^2}{\beta\Delta T} \tag{67}$$

$$\mathrm{Bi} \stackrel{\text{def}}{\equiv} 2\left(\frac{b^2}{t_d^2}\right)\frac{h_d t_d}{k_d} \tag{68}$$

The modified Biot number Bi can be related to the rotational Reynolds number as

$$\mathrm{Bi} = \frac{2}{\pi}\left(\frac{b}{t_d}\right)\left(\frac{k}{k_d}\right)\mathrm{Re}_\phi^{1/2} \tag{69}$$

As buoyancy-induced flow is a conjugate problem, the properties of the disc material have a significant effect on the temperatures of the disc and core.

The compressibility parameter χ depends on compressible flow in the air; as shown below, the core temperature increases as χ increases. The λ parameter is related to convection from the discs and shroud to the air; for the closed cavity cases considered here, χ is several orders of magnitude larger than λ. For a closed cavity with adiabatic discs, the first term in eq. (63) vanishes and the core temperature rise can be calculated through integrating eq. (63), hence

$$\theta_{c,b} - \theta_{c,a} = \frac{1}{2}(1 - x_a^2)(\gamma - 1)\chi \tag{70}$$

For cavity air with $\gamma = 1.4$ and hub radius $x_a = a/b = 0.5$, $\theta_{c,b} - \theta_{c,a} = \theta_{d,b} - \theta_{d,a} = 1$ when $\chi \approx 6.7$. This means that, if $T_b = T_s$, above this critical value the core temperature near the shroud exceeds the shroud temperature. *There will be no convective heat transfer from the shroud, and the flow in the closed cavity will be no longer buoyancy-induced and can become stratified.*

For buoyancy-induced flow and heat transfer, empirical relationships are used below for Nu_s, Nu_h and C_w, where the subscripts h and s denote the hub and shroud respectively. From the model of Tang and Owen [25] for buoyancy-induced flow in a closed cavity, from the experimental study in [26], the shroud Nusselt number was assumed to be equivalent to that for laminar free convection from a horizontal plate but with the gravitational acceleration replaced by the centripetal acceleration at the shroud surface, so that

$$Nu_s = C(Gr_s Pr)^{1/4} \tag{71a}$$

$$Nu_h = C(Gr_h Pr)^{1/4} \tag{71b}$$

where the Grashof numbers are defined as

$$\mathrm{Gr}_s \stackrel{\text{def}}{\equiv} \rho_{c,b}^2 \Omega^2 b\left(\frac{s}{2}\right)^3 \beta\left(T_s - T_{c,b}\right)/\mu^2 \tag{72a}$$

$$\mathrm{Gr}_h \stackrel{\text{def}}{\equiv} \rho_{c,a}^2 \Omega^2 a(\frac{s}{2})^3 \beta\left(T_{c,a} - T_h\right)/\mu^2 \tag{72b}$$

For the results evaluated below, the correlations in [25] were used, where C = 0.32.

From eq. (59), the plume mass flow parameter and the pressure parameter can be related using

$$C_w = \frac{1}{2} n \mathrm{Re}_\phi C_p \tag{73}$$

There is no accepted correlation for C_w, the mass flow rate in the plumes, and so the equation used to correlate the data in [14] of this paper is used here, where

$$C_w = 1.0(\mathrm{Gr}_s \mathrm{Pr})^{0.61} \tag{74}$$

As stated above, the compressibility parameter χ has a strong effect on the core temperatures. The core temperatures in turn influence the disc temperatures. The disc temperature also depends on Bi, where, as shown by eq. (69), for constant disc properties, $\mathrm{Bi} \propto Re_\phi^{1/2}$. Consequently, Re_ϕ, $\beta\Delta T$ and χ (or Re_ϕ, $\beta\Delta T$ and Ma) can be thought of as *the three independent variables* that control these temperatures. (The reader familiar with free convection might well ask the question: where is Gr, the Grashof number? To quote "Napoleon: You have written this huge book on the system of the world without once mentioning God. Laplace: Sire, I had no need of that hypothesis.")

As discussed in Section 1, in a rotating frame of reference, where the gravitational acceleration is replaced by the centripetal acceleration, $\mathrm{Gr} \stackrel{\text{def}}{\equiv} \mathrm{Re}_\phi{}^2 \beta\Delta T$, So, if the temperatures can be described in terms of the three parameters Re_ϕ, $\beta\Delta T$ and χ then they can also be described, for example, in terms of the appropriate combination of χ and any two of the three parameters Re_ϕ, $\beta\Delta T$ and Gr. *The important thing to note is that, in compressible rotating fluids, the temperatures of the disc and core do not depend solely on any single parameter.*

For the cases discussed below, the effects of all relevant parameters are considered.

5.2 Solution techniques

A diagram of the closed cavity used in this study is shown in Figure 4. It is assumed that $T_a = T_h$, and $T_b = T_s$, also that a = 120 mm, b = 240 mm, s = 40 mm *(x_a = a/b = 0.5, s/(b-a) = 0.33)*, and the disc thickness, t_d, is 8 mm. Different

Journal of Turbomachinery. Received July 17, 2022;
Accepted manuscript posted August 25, 2022. doi:10.1115/1.4055449

rotational speeds and different temperature differences ($T_b - T_a$) are considered, while the hub temperature T_a is fixed at 300K. The stationary isothermal cavity is assumed to be filled with air where T_o= 300 K and p_o = 1 bar, and μ, c_p and k are evaluated at the temperature of $(T_a + T_b)/2$. The back face of the disc is thermally insulated (as is the case for the experimental discs in Part 2); this is equivalent to a disc of 16 mm thickness with equal heat transfer from the two surfaces. The disc thermal conductivity is assumed to follow $k/k_d = 0.01$, which is similar to that of titanium alloy.

As heat transfer in closed rotating cavities is a conjugate problem, the core and disc temperatures are coupled. They can be calculated by solving eqs. (33) and (36) iteratively until the heat balance for the closed cavity system is reached, so that

$$\dot{Q}_s + \dot{Q}_d = \dot{Q}_h \tag{75}$$

where $\dot{Q}_s$, $\dot{Q}_h$ and $\dot{Q}_d$ are the heat flow from the shroud surface, the hub surface and both disc surfaces, respectively. $\dot{Q}_s$ and $\dot{Q}_h$ can be calculated using eqs. (29) and (35). The shroud and hub heat transfer coefficients, h_s and h_h, can be determined from the correlations provided in section 5.1. The disc heat flow $\dot{Q}_d$ is calculated by integrating $d\dot{Q}_d$ (see eq. 26) from a to b.

An initial guess is needed for the distribution of the core temperature, which is assumed to equal the hub temperature T_h. For each calculated core temperature distribution, the pressure distribution can be determined using eqs. (40) and (48), and the disc temperature distribution can be obtained by solving eq. (36). A Crank-Nicolson scheme together with the Dirichlet boundary conditions, $T_a = T_h$ and $T_b = T_s$, were employed. Once the disc temperatures are calculated, the heat flux from the discs, shroud and hub can be evaluated. The heat balance equation, eq. (75), can then be checked, and this can be used to update the core temperature at the inner radius, $T_{c,a}$. Eq. (33) is then solved to update the radial distribution of the core temperature. Iteration is continued until the sum of all heat flows reduces to a tolerance of 0.01 W. The solution process is illustrated in Figure 5.

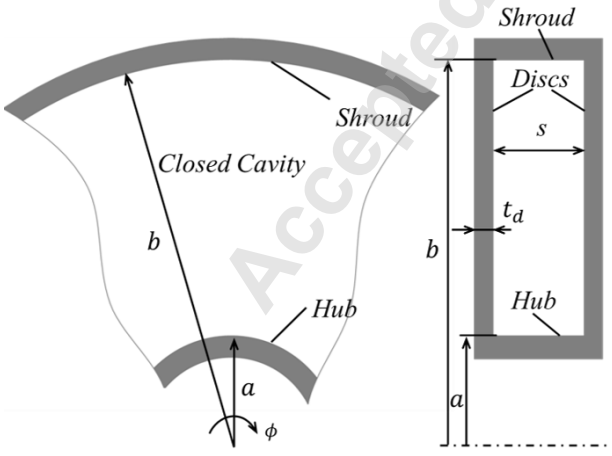

Figure 4: Geometry used for calculation of disc and core temperatures. Left: *r-Φ* view. Right: *r-z* view.

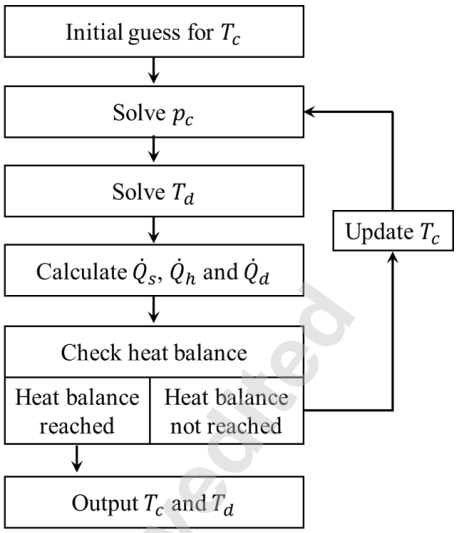

Figure 5: Solution process to solve core and disc temperatures

5.3 Calculated temperatures and fluxes

The values of all parameters for the cases considered are given in Table 1.

Figure **6** shows the calculated distributions of the non-dimensional disc, core and plume temperatures for cases A_1 and C_1. For both cases, the disc temperature is higher than the core temperature in the outer region and lower in the inner region. The difference between the plume temperatures decreases as Gr, and consequently the mass flow rate in the plumes, increases. This temperature difference also decreases as χ, and consequently the core temperature, increases. Both these effects explain why the difference between the plume temperatures is larger in case A_1 than that in C_1.

Case No.	N (rpm)	Re_ϕ	$\beta\Delta T$	Gr	Ma	χ
A_1	4000	1.4×10^6	0.15	2.9×10^{11}	0.28	0.52
A_2	4000	1.4×10^6	0.040	8.8×10^{10}	0.28	2.1
A_3	4000	1.4×10^6	0.019	4.0×10^{10}	0.28	4.7
B_1	8000	2.8×10^6	0.15	1.2×10^{12}	0.56	2.1
C_1	12000	4.2×10^6	0.15	2.6×10^{12}	0.84	4.7
C_2	12000	4.2×10^6	0.30	5.0×10^{12}	0.84	2.1

Table 1: Parameters for the cases considered below

It should be noted that, for case C_1 in Figure **6**, there is only a small difference between the temperatures of the shroud and the core at r = b. As discussed in section 5.1, there will be a critical value of χ where the core temperature equals that of the shroud, and the critical χ is 6.7 if both discs are adiabatic. This value can be changed by the disc heat transfer and the cavity geometry. Although the theoretical model is invalid above this critical value, and conduction in the core is not included in the model, it is reasonable to speculate that *stratification* of the core will

Journal of Turbomachinery. Received July 17, 2022;
Accepted manuscript posted August 25, 2022. doi:10.1115/1.4055449

occur. This, as discussed in Section 1, is where buoyancy-induced convection cannot occur and heat transfer from shroud to the core is reduced to conduction. This large reduction of heat transfer, which could occur during an engine cycle, would have a significant effect on the temperature of the compressor discs.

Figure 7 shows the ratio of disc to shroud heat flux, q_d/q_s, for cases A_1 and C_1. It can be seen that although the disc flux increases with radius, the flux ratio is positive (indicating heat transfer from the disc to the core) in the outer part of the cavity and negative in the inner part. This flux reversal, which is consistent with the difference between the disc and core temperatures in

Figure **6**, was observed from experimental measurements in [14].

5.4 Effect of Re_ϕ, χ and $\beta\Delta T$

As pointed out in Section 5.1, the effect of the compressibility on both θ_c and θ_d increases as χ increases, and the disc temperature θ_d is also affected by the Biot number hence the rotational Reynolds number Re_ϕ. Figure 8 shows the effect of χ on the radial distribution of the disc and core temperatures at a fixed rotational Reynolds number of $\mathrm{Re}_\phi = 1.4 \times 10^6$ (cases A_1, A_2 and A_3 in Table 1). It can be seen that at the higher radii the core temperature approaches that of the shroud as χ increases. This will reduce the temperature difference hence the heat transfer between the disc and the core, leading to higher disc temperatures near the shroud and lower ones near hub. Figure 9 shows the effect of Re_ϕ on the radial distribution of the disc and core temperatures at a fixed value of χ = 2.1(cases A_2, B_1 and C_2 in Table 1). As Re_ϕ increases, there are no significant changes of the core temperatures, but the disc temperature decreases monotonically at the higher radii due to the increase of Biot numbers.

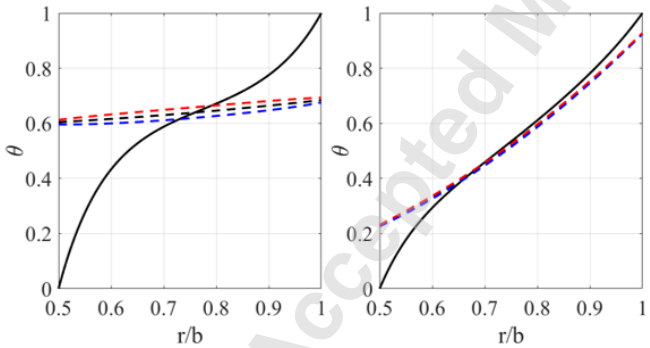

(a) case A_1 ($\mathrm{Re}_\phi \approx 1.4 \times 10^6, \chi = 0.52$) (b) case C_1 ($\mathrm{Re}_\phi \approx 4.2 \times 10^6, \chi = 4.7$)

Figure 6: Disc, core and plume temperatures for βΔT=0.15. Solid lines denote disc temperatures; red, blue and black broken lines denote hot plume, cold plume and core temperatures.

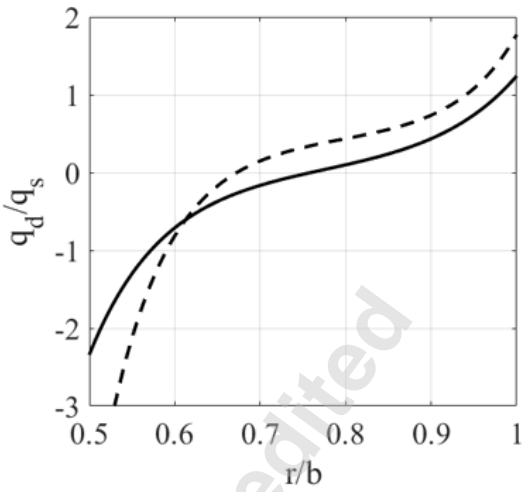

Figure 7: Heat flux ratio for cases A1 (solid curve) and C1 (broken curve).

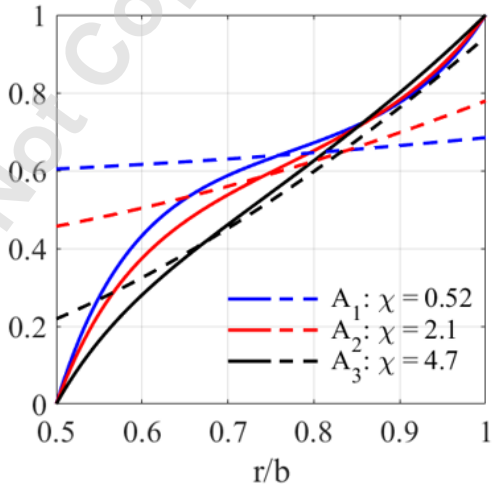

Figure 8: Effect of χ on disc and core temperatures for $\mathrm{Re}_\phi \approx 1.4 \times 10^6$. Solid lines denote disc temperatures; broken lines denote core temperatures.

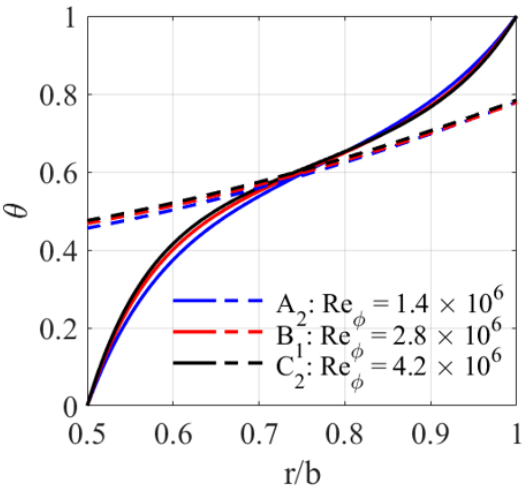

Figure 9: Effect of Re_ϕ on disc and core temperatures for $\chi \approx 2.1$. Solid lines denote disc temperatures; broken lines denote core temperatures.

Journal of Turbomachinery. Received July 17, 2022;
Accepted manuscript posted August 25, 2022. doi:10.1115/1.4055449

5.5 Effect of disc thermal conductivity on disc temperatures

Although Bi can be varied by changing Re_ϕ, more significant changes occur as a result of the thermal conductivity of the disc material k_d. Figure 10 shows the effect of the disc conductivity on the radial distribution of the disc temperature. For the smaller values of conductivity, most of the radial variation of disc temperature is confined to regions close to the shroud and hub. However, as the thermal conductivity increases, the disc temperature gradient also increases, and in the limiting case it approaches the distribution corresponding to one-dimensional radial conduction in a cylinder, where

$$\theta_d = \frac{\ln(r/r_a)}{\ln(r_b/r_a)} \tag{76}$$

This corresponds to the solution of eq. (64) when Bi = 0.

This parametric study and that in section 5.4 show the theoretical effects of the flow parameters and the disc conductivity on the temperature distributions of the disc and core. The practical effects will also depend on the assumptions made for the heat flux from the shroud and hub and on the geometry of the cavity. In [14], the theoretical values of the temperature distributions are compared with measurements made in an experimental rig.

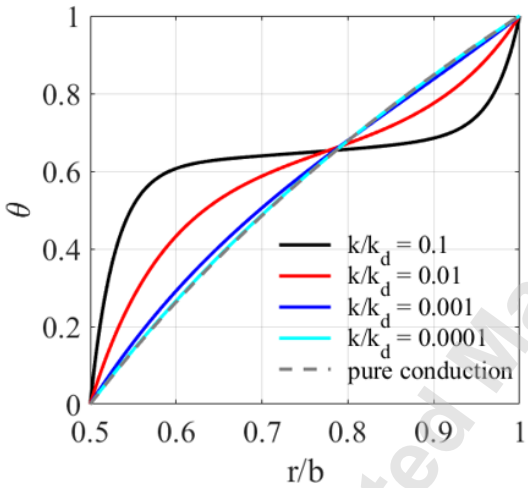

Figure 10: Effect of disc thermal conductivity on disc temperatures ($\mathrm{Re}_\phi = 1.4 \times 10^6$, $\beta\Delta T = 0.15$, *and* $\chi = 0.52$)

6 CONCLUSIONS

A theoretical model has been developed to calculate the radial distribution of the temperature of the discs and fluid core for buoyancy-induced flow in a closed rotating cavity. The principal assumptions are that the convective heat transfer from the hot shroud to the cold hub is via plumes of fluid in which the cold fluid moves radially outward, and the hot fluid inward, inside an inviscid quasi-axisymmetric core of rotating fluid in which there are radial and circumferential distributions of pressure. The fluid core is surrounded by boundary layers on all rotating surfaces, with thin free-convection layers on the surfaces of the shroud and hub and laminar Ekman layers on the surface of the discs, from where heat is convected to the core. In addition to the convection, heat is transferred by one-dimensional radial conduction in the rotating discs. As the equations for the convection in the fluid and the conduction in the discs are coupled, this makes it a conjugate problem.

Using the model, equations have been derived to calculate the radial distribution of temperature in the discs and fluid core. These equations reveal that the non-dimensional temperatures for the disc and core, θ_d and θ_c, are controlled by three independent non-dimensional parameters: Re_ϕ, $\beta\Delta T$ and χ, the rotational Reynolds number, the buoyancy parameter, and the compressibility parameter respectively. Importantly, the core temperature is shown to depend strongly on the value of χ. (If required, the Grashof number could be used to replace either Re_ϕ or $\beta\Delta T$ as one of the three independent parameters.) Additional equations derived for the radial pressure gradient in the rotating core show that the pressure depends not only on the rotational speed and temperature distribution of the core but also on the initial values of pressure and density in the stationary isothermal cavity. It is also shown that the mass flow rate in the plumes is proportional to the circumferential pressure gradient in the core.

A parametric study has been conducted to show the effect of Re_ϕ, $\beta\Delta T$ and χ on the radial distributions of θ_d and θ_c for a closed rotating cavity where the radius ratio, a/b, equals 0.5 and the thermal conductivity of the discs corresponds to that of titanium. The closure of the equations requires an overall heat balance in which the heat transferred from the shroud and discs into the fluid equals the heat transferred from the fluid to the hub. Heat transfer for the shroud and hub was calculated using a laminar free-convection model, which had previously been validated using published experimental data. Although other free convection models would result in different quantitative results, they are not expected to make any significant qualitative difference to the principal conclusions presented here.

The study shows that θ_c depends strongly on χ and that θ_d depends on Re_ϕ and θ_c. For small values of χ, there is no significant change of θ_c and, at the higher radii, θ_d decreases as Re_ϕ increases. For large values of χ, typical of those found in engines, at *the higher radii* the temperature of the core approaches that of the shroud; this reduces the heat transfer from the disc and shroud and increases θ_d. There will be a critical value of χ at which the core temperature equals that of the heated shroud; above this critical value, stratification is expected to occur and heat transfer from the shroud to the core will be by conduction rather than by convection. For a closed cavity with a/b = 0.5 and adiabatic discs, this critical value is 6.7. This stratification could have a significant effect on the temperature distribution of a compressor disc during a flight cycle.

Different disc thermal conductivities were used to show that as the conductivity of the discs is increased the radial distribution of disc temperature tends to that for one-dimensional conduction in a solid cylinder.

Predictions from the model are shown to be in good agreement with experimental measurements in the companion paper [14].

NOMENCLATURE

a	inner radius of cavity (hub) (m)
b	outer radius of cavity (shroud) (m)
c	speed of sound in cavity (m/s)
c_p	specific heat capacity ($=\sqrt{\gamma R(T_b+T_a)/2}$) (J/(kgK))
C	constant for shroud and hub heat transfer
d	vertical distance between the plates (m)
g	gravitational acceleration (m/s^2)
h	heat transfer coefficient (W/(m^{2}K))
H	specific total enthalpy (m^2/s^2)
k	thermal conductivity of air (W/(mK))
k_d	thermal conductivity of disc (W/(mK))
m	total mass in the closed cavity (kg)
$\dot{m}$	mass flow rates in plumes (kg/s)
n	number of vortex pairs
N	rotational speed
p	pressure (Pa)
q	heat flux (W/ m^2)
$\dot{Q}$	heat flow rate (W)
r	radius (m)
R	specific gas constant (J/(kgK))
s	axial space between discs in cavity (m)
t_d	thickness of disc (m)
T	temperature (K)
u, v	relative velocity (m/s)
U	absolute velocity (m/s)
V	volume of the cavity (m^3)
$\dot{W}$	work flow rate(W)
x	nondimensional radius ($=r/b$)
z	axial coordinates (m)
β	volume expansion coefficient($=1/(T_a/2+T_b/2)$)(K^{-1})
δ	Ekman layer thickness (m)
Δp	pressure difference between vortices (Pa)
ΔT	temperature difference (=T_b-T_a) (°C)
λ	nondimensional parameter related to disc heat transfer
μ	dynamic viscosity (kg/(ms))
η	radial inflow direction (m)
ρ	density (kg/m^3)
ϕ	circumferential angle in core
φ	axial angle in Ekman layers
Ω	angular speed of disc (s^{-1})

Dimensionless parameters

Bi	modified Biot number ($\stackrel{\text{def}}{=} 2\left(\frac{b^2}{t_d^2}\right)\frac{h_d t_d}{k_d}$)
C_w	plume mass flow parameter ($\stackrel{\text{def}}{=} \frac{\dot{m}}{\mu s}$)
C_p	pressure coefficient ($\stackrel{\text{def}}{=} \frac{\Delta p}{\rho_o \Omega^2 b^2}$)
Gr	Grashof number
Ma	rotational Mach number ($\stackrel{\text{def}}{=} \Omega b/c$)
Nu	Nusselt number
Pr	Prandtl number
Ra	Rayleigh number for rotating cavities ($\stackrel{\text{def}}{=}$ GrPr)
Ra′	Rayleigh number for stationary case
Re_ϕ	rotational Reynolds number ($\stackrel{\text{def}}{=} \rho_o \Omega b^2/\mu$)
θ	nondimensional temperature for fin ($\stackrel{\text{def}}{=} (T-T_a)/(T_b-T_a)$)
χ	compressibility parameter ($\stackrel{\text{def}}{=}$ Ma$^2/\beta\Delta T$)

Subscripts

a	value at $r = a$
b	value at $r = b$
c	values in core
$crit$	critical values
C	cold plate
d	values in disc
h	value on hub surface
H	hot plate
i	index for plumes
o	initial value
$\hat{p}, \check{p}$	values of cold and hot plumes
s	value on shroud surface
z, r, ϕ	axial, radial, circumferential direction
∞	local values in fluid core

References

[1] Owen, J. M., and Long, C. A., 2015, "Review of Buoyancy-Induced Flow in Rotating Cavities," ASME J. Turbomach., 137(11), p. 111001.
[2] Tritton, D. J., 1988, Physical Fluid Dynamics, OUP, New York.
[3] Owen, J. M., 2010, "Thermodynamic Analysis of Buoyancy-Induced Flow in Rotating Cavities," ASME J. Turbomach., 132(3), p. 031006.
[4] Jackson, R. W., Tang, H., Scobie J. A., Owen J. M. and Lock G. D., 2021, "Measurement of Heat Transfer and Flow Structures in a Closed Rotating Cavity," ASME Paper No. GT2021-59605.
[5] Farthing, P. R., Long, C. A., Owen, J. M., and Pincombe, J. R., 1992, "Rotating Cavity with Axial Throughflow of Cooling Air: Flow Structure," ASME J. Turbomach., 114(1), pp. 237–246.
[6] Bohn, D., Deutsch, G., Simon, B., and Burkhardt, C., 2000, "Flow Visualisation in a Rotating Cavity with Axial Throughflow," ASME Paper No. 2000-GT-0280.
[7] Miché, N. D., 2009, "Flow and Heat Transfer Measurements inside a Heated Multiple Rotating Cavity with Axial Throughflow", PhD thesis, University of Sussex, UK.
[8] Long, C. A., Miche, N. D. D., and Childs, P. R. N., 2007, "Flow Measurements Inside a Heated Multiple Rotating Cavity with Axial Throughflow," Int. J. Heat Fluid Flow, 28(6), pp. 1391–1404.
[9] Jackson, R. W., Tang, H., Pountney, O. J., Scobie, J. A., Sangan, C. M., Owen, J. M., and Lock, G. D., 2021, "Unsteady Pressure Measurements in a Heated Rotating Cavity," ASME Paper No. GT2021-59090.
[10] Tucker, P. G., 2002, "Temporal Behaviour of Flow in Rotating Cavities," Numer. Heat Transfer A, 41(6–7), pp. 611–627.

[11] Bohn, D., Ren, J., and Tuemmers, C., 2006, "Investigation of the Unstable Flow Structure in a Rotating Cavity," ASME Paper No. GT2006-90494.
[12] King, M. P., Wilson, M., and Owen, J. M., 2007, "Rayleigh–Benard Convection in Open and Closed Rotating Cavities," ASME J. Eng. Gas Turbines Power, 129(2), pp. 305–311.
[13] Sun, X., Linblad, K., Chew, J. W., and Young, C., 2007, "LES and RANS Investigations into Buoyancy-Affected Convection in a Rotating Cavity with a Central Axial Throughflow," ASME J. Eng. Gas Turbines Power, 129(2), pp. 318–325.
[14] Lock, G. D., Jackson, R. W., Pernak, P., Pountney, O. J., Sangan, C. M., Owen, J. M., Tang, H., and Scobie, J. A., 2022, "Stratified and Buoyancy-Induced Flow in Closed Compressor Rotors", ASME Paper GT2022-82023.
[15] Owen, J. M., and Tang H., 2015, "Theoretical Model of Buoyancy-Induced Flow in Rotating Cavities," ASME J. Turbomach., 137(11), p. 111005.
[16] Tang, H., and Owen, J. M., 2017, "Effect of Buoyancy-Induced Rotating Flow on Temperature of Compressor Discs," ASME J. Eng. Gas Turbines Power, 139(6), p. 062506.
[17] Tang, H., Puttock-Brown, M. R., and Owen, J. M., 2018, "Buoyancy-Induced Flow and Heat Transfer in Compressor Rotors," ASME J. Eng. Gas Turbines Power, 140(7), p. 071902.
[18] Jackson, R. W., Luberti, D., Tang, H., Pountney, O. J., Scobie, J. A., Sangan, C. M., & Lock, G. D., 2021, "Measurement and Analysis of Buoyancy-Induced Heat Transfer in Aero-Engine Compressor Rotors," ASME J. Eng. Gas Turbines Power, 143(6), 061004.
[19] Pitz, D. B., Chew, J. W., & Marxen, O., 2019, "Effect of an Axial Throughflow on Buoyancy-Induced Flow in a Rotating Cavity," Int. J. Heat Fluid Flow, 80, 108468.
[20] Gao, F., Pitz, D. B. and Chew, J. W., 2020, "Numerical Investigation of Buoyancy-Induced Flow in a Sealed Rapidly Rotating Disc Cavity," Int. J. Heat Mass Transfer, 147, 118860.
[21] Hickling, T., & He, L., 2021, "Some Observations on the Computational Sensitivity of Rotating Cavity Flows," ASME J. Eng. Gas Turbines Power, 143(4), 041014.
[22] Owen, J. M., and Rogers, R. H., 1995, Flow and Heat Transfer in Rotating Disc Systems, Volume 2—Rotating Cavities, Research Studies Press, Taunton, UK.
[23] Childs, P. R. N., 2011, Rotating Flow, Elsevier, Oxford, UK.
[24] Tang, H., Shardlow, T., and Owen, J. M., 2015, "Use of Fin Equation to Calculate Nusselt Numbers for Rotating Disks," ASME. J. Turbomach., 137(12), p. 121003.
[25] Tang, H., and Owen, J. M., 2018, "Theoretical Model of Buoyancy-Induced Heat Transfer in Closed Compressor Rotors," ASME J. Eng. Gas Turbines Power, 140(3), pp. 032605.
[26] Bohn, D., Deuker, E., Emunds, R., and Gorzelitz, V., 1995, "Experimental and Theoretical Investigations of Heat Transfer in Closed Gas Filled Rotating Annuli," ASME J. Turbomach., 117(1), pp. 175–183.